Development of Polyurethanes with Azo-Type Chromophores for Second-Order Nonlinear Optical Applications

S. M. Tambe,[1] R. G. Tasaganva,[1] J. J. Jogul,[2] D. C. Castiglione,[3] M. Y. Kariduraganavar[1]

[1]Department of Chemistry and Center of Excellence in Polymer Science, Karnatak University, Dharwad 580 003, India
[2]Department of Chemistry, Kittel Science College, Dharwad 580 001, India
[3]Department of Chemistry, University of Reading, Reading RG6 6AD, United Kingdom

ABSTRACT: Active nonlinear optical nitro-substituted thiazole, benzothiazole, and thiadiazole chromophores were prepared and condensed with tolylene-2,4-diisocyanate (TDI) and 4,4′-methylenedi(phenyl isocyanate) (MDI) to yield a series of polyurethanes. The resulting polyurethanes were characterized with Fourier transform infrared, proton nuclear magnetic resonance, and ultraviolet–visible spectroscopy, differential scanning calorimetry, thermogravimetric analysis, and gel permeation chromatography. The weight-average molecular weights of the polyurethanes ranged between 19,500 and 28,000 (weight-average molecular weight/number-average molecular weight = 1.71–2.15). All the polyurethanes exhibited excellent solubility in most common organic solvents, and this indicated that these polyurethanes offered good processability. The glass-transition temperatures (T_g's) of the polyurethanes were in the range of 166–204°C. Among the polyurethanes, chromophores containing the nitrothiazole moiety exhibited lower T_g values in comparison with those of chromophores containing nitrobenzothiazole and nitrothiadiazole moieties. This was attributed to the small size of the nitrothiazole moiety in the polyurethane matrix. The polyurethanes containing a TDI backbone demonstrated relatively high T_g values in comparison with those of the polyurethanes containing an MDI backbone. This was a result of an enhancement of the rigidity caused by the incorporation of a toluene ring into the polyurethane backbone. The second harmonic generation (SHG) coefficients of the poled polyurethane films ranged from 67.29 to 105.45 pm/V at 1064 nm. High thermal endurance of the poled dipoles was observed for all the polyurethanes. This was attributed to the formation of extensive hydrogen bonds between urethane linkages. Furthermore, none of the developed polyurethanes showed SHG decay below 150°C, and this signified their acceptability for nonlinear optical devices. © 2009 Wiley Periodicals, Inc. J Appl Polym Sci 114: 2291–2300, 2009

Key words: azo polymers; differential scanning calorimetry (DSC); NLO; thermogravimetric analysis (TGA)

INTRODUCTION

Nowadays, the design of new materials exhibiting higher second-order nonlinear optical (NLO) efficiency is attracting a great deal of interest.[1–3] This is mainly because of their potential applications in optical signal processing, data storage, and sensors in photonic-based industries, among other things.[4–6] In this respect, remarkable attention has been paid to polymers as the basic constituents of organic materials exhibiting second-order NLO properties, and polymers offer many advantages, such as considerably easy preparation, fabrication, and molding. In addition, they are lightweight and have mechanical endurance, chemical resistance, and good processability for preparing optical devices.[7,8]

Generally, when new NLO materials are being designed, the intrinsic NLO efficiency of the chromophore segments is mainly considered a relevant parameter. Recently, it has been proved that the introduction of aromatic heterocyclic rings along the conjugation path results in increased hyperpolarizability in comparison with all benzenoid systems.[9–11] This is due to the delocalization energy of heteroaromatics, which is lower than that of six-membered rings. Chromophores containing aromatic pentaatomic heterocycles or their derivatives, such as thiophene,[12–14] thiazole,[15,16] benzothiazole,[16,17] and benzoxazole,[18,19] are among the most studied systems. In addition, it is also necessary to give primary importance to other ancillary properties that may play an important role by influencing material processing and performance (e.g., film making, poling deficiency, durability, and thermal and photochemical stability).[19,20] To achieve these goals, several strategies have been proposed recently. Extensively crosslinked polymeric matrices[21–24] and high-glass-transition materials such as polyimides[25–29] have

Correspondence to: M. Y. Kariduraganavar (mahadevappak@yahoo.com).

been studied to suppress the orientational relaxation at higher operating temperatures. The most recent strategy for satisfying high orientational stability is the development of NLO polymers, whose dipole moments align transversely to the polymer backbone.[30–32]

In this series of NLO polymers, polyurethanes with NLO chromophores have been found to be promising candidates whose dipole moments are aligned transversely to the main-chain backbones, exhibiting large second-order nonlinearity with good thermal stability.[30,31,33] Furthermore, systems pseudo-crosslinked via hydrogen bonds have advantages such as homogeneity and good processability in comparison with chemically crosslinked systems, which suffer from significant optical loss and poor processability. It has also been reported[31,34] that crosslinked polyurethanes with azo-benzene chromophores show enhanced thermal stability as the polymer matrix forms extensive hydrogen bonds between urethane linkages and thereby increases the rigidity, preventing the relaxation of induced dipoles.[35–39]

In this work, we chose polyurethanes as the polymer backbones; they have moderate glass-transition temperature (T_g) values and structures that allow pseudo-crosslinking with interchain hydrogen bonds. Strong secondary forces between polymer chains are expected to increase the rigidity of the matrix and prevent the randomization processes of the oriented chromophore dipoles. To enhance the optical nonlinearity, azo-type chromophores with thiazole, benzothiazole, and thiadiazole as strong acceptors were introduced into the polyurethane backbones. After confirmation of the structures of the resulting polyurethanes, the nonlinear properties and thermal orientation stability of the poled polyurethanes embedded with the aforementioned chromophores were explored.

EXPERIMENTAL

Materials

2-Amino-5-nitrothiazole, 2-amino-6-nitrobenzothiazole, tolylene-2,4-diisocyanate (TDI), 4,4′-methylene-di(phenyl isocyanate) (MDI), and N-phenyldiethanolamine were purchased from Sigma–Aldrich (Steinheim, Germany). N,N-Dimethylformamide (DMF) was procured from Loba Chemie (Mumbai, India) and purified by distillation over phosphorous pentoxide. 4-Nitrobenzoic acid, phosphorous oxychloride, and thiosemicarbazide were purchased from S. D. Fine Chemicals, Ltd. (Mumbai, India). All other chemicals were analytical-grade and were purchased from S. D. Fine Chemicals; they were used as received unless otherwise stated.

Instruments

Fourier transform infrared (FTIR) spectra were recorded on a Nicolet (Madison, WI) 5700 spectrometer. The proton nuclear magnetic resonance (^{1}H-NMR) spectra were recorded on a Bruker (Faellanden, Switzerland) Avance 300-MHz spectrometer with tetramethylsilane as a reference. The number-average molecular weight (M_n) and weight-average molecular weight (M_w) values of the polyurethanes were estimated by high-performance gel permeation chromatography (GPC; Waters, Milford, MA). Degassed tetrahydrofuran (THF) was used as the eluent at a flow rate of 1.0 mL/min. A set of monodisperse polystyrene (PS) standards covering the range of 10^3–10^7 was used for the molecular weight calibration. Elemental analyses were performed with a PerkinElmer (Norfolk, CT) PE 2400 CHN elemental analyzer. Ultraviolet–visible (UV–vis) spectra were recorded on a Hitachi (Kowloon, Hong Kong) U-2800 spectrophotometer. Differential scanning calorimetry (DSC) and thermogravimetric analysis (TGA) were performed on a Mettler–Toledo (Zurich, Switzerland) DSC 822e and a PerkinElmer Diamond TGA/DTA thermogravimetric analyzer under nitrogen at a heating rate of 10°C/min. The melting points were measured with open capillary tubes on a melting point apparatus. Thin polymer films were produced from a 5 wt % solution of the polymer in DMF on an indium tin oxide glass substrate by a spin-casting technique at a rate of approximately 1500–2000 rpm. Before the film casting, the polymer solution was filtered through a 0.20-μm Teflon membrane filter. All films were dried for 3 h in a vacuum oven at 100°C to remove residual solvents. The thickness and refractive indices of the polyurethanes were measured with an SE 850 ellipsometer (Berlin, Germany).

Second harmonic generation (SHG) measurements

The dried film was heated 10°C below T_g and corona-poled with an intense dc electric field as described in our earlier article.[40] After being poled for 1 h, the polyurethane film was cooled to room temperature in the presence of an electric field. The poling conditions were as follows: a high voltage of 3 kV at the needle point, a gap distance of about 0.8 cm, and a poling current less than 0.18 mA.

The second harmonic measurements were performed with a setup described previously.[40] A mode-locked Nd:YAG laser (Minilite-I, Continuum, Santa Clara, CA; 6-ns pulse duration, 28-mJ maximum energy, and 10-Hz repetition rate at 1064 nm) was used as a fundamental light source. The second harmonic signal generated by the p-polarized fundamental wavelength (1064 nm) was detected by a fast photodiode (FDS010, Thorlabs, Newton, NJ; 0.9-ns rise time) and a digital phosphor oscilloscope (TDS 724D, Tektronix, Beaverton, OR). The polymer

sample was held at a 45° angle to the incident laser beam. A standard KDP crystal was used as a reference sample. The chromophore alignment in the polyurethane films and the second-order NLO properties were described by an order parameter.

Synthesis of the chromophores

Synthesis of chromophore a

Dry sodium nitrite (0.34 g, 5 mmol) was added slowly to concentrated sulfuric acid (18 mL) with stirring and was warmed to 50°C with a water bath. The solution was cooled to 0°C, and glacial acetic acid (22 mL) was added dropwise with stirring while the temperature was maintained below 15°C. The resulting solution was cooled below 0°C, and to this, 2-amino-5-nitrothiazole (0.73 g, 5 mmol) was added portionwise with stirring. The stirring was continued at this temperature for 2 h. The resulting reaction mixture was poured into crushed ice to obtain a diazonium salt solution, which was slowly poured into a methanol/water (10 mL/5 mL) mixture containing N-phenyldiethanolamine (0.91 g, 5 mmol). The reaction temperature was maintained below 0°C. After stirring for 1 h, the mixture was neutralized with 50% ammonia. The resulting precipitate was filtered and washed several times with water until the filtrate was neutral. The product was purified by column chromatography over SiO_2 with benzene and ethyl acetate (1:1) as an eluate, and this resulted in pure a with a 0.58-g yield (35%).

mp: 143–145°C. Maximum absorption wavelength (λ_{max}; DMF): 583 nm. ^{1}H-NMR [hexadeuterated dimethyl sulfoxide (DMSO-d_6), ppm, δ]: 3.70 (m, 8H), 4.91 (s, 2H), 7.08 (d, 2H), 7.80 (d, 2H), 8.78 (s, 1H). FTIR (KBr, cm^{-1}): 3393 (s, O—H), 2924, 2842 (m, C—H), 1602 (s, N=N), 1520, 1334 (vs, N=O). ANAL. Calcd for $C_{13}H_{15}N_5O_4S$: C, 46.29%; H, 4.45%; N, 20.77%. Found: C, 46.05%; H, 4.23%; N, 20.57%.

A similar procedure was followed for the synthesis of chromophore b.

Synthesis of chromophore b

Yield: 65%. mp: 215–216°C. λ_{max} (DMF): 541 nm. ^{1}H-NMR (DMSO-d_6, δ): 4.14 (br s, 8H), 4.93 (s, 2H), 6.64 (d, 2H), 7.33 (d, 2H), 8.00 (t, 2H), 8.48 (s, 1H). FTIR (KBr, cm^{-1}): 3366 (s, O—H), 2918, 2853 (m, C—H), 1596 (s, N=N), 1503, 1340 (vs, N=O). ANAL. Calcd for $C_{17}H_{17}N_5O_4S$: C, 52.71%; H, 4.39%; N, 18.08%. Found: C, 52.53%; H, 4.28%; N, 18.19%.

Synthesis of chromophore c

Before the synthesis of chromophore c, 2-amino-5-(4-nitrophenyl)-1,3,4-thiadiazole was prepared according to the procedure described by Foroumadi et al.[41] A mixture of p-nitrobenzoic acid (4.2 g, 0.025 mol), thio-

semicarbazide (2.25 g, 0.025 mol), and phosphorous oxychloride (10 mL) was refluxed gently for 30 min at 80°C. After cooling, water (25 mL) was added, and the resulting mixture was refluxed further for 4 h at 100°C and filtered. The filtrate was neutralized with a 10% KOH solution. The obtained precipitate was filtered and washed several times with water until the pH of the filtrate was 7. It was then recrystallized from ethanol. The analytical and spectral data were in good agreement with previously reported data.[41]

This compound was used for the preparation of chromophore c according to the procedure adopted for chromophore a.

Yield: 59%. mp: 160–161°C. λ_{max} (DMF): 544 nm. ^{1}H-NMR (DMSO-d_6, δ): 3.33 (br s, 8H), 4.96 (s, 2H), 7.00 (d, 2H), 7.83 (d, 2H), 8.30 (d, 2H), 8.38 (d, 2H). FTIR (KBr, cm^{-1}): 3388 (s, O—H), 2913, 2847 (m, C—H), 1596 (s, N=N), 1509, 1351 (vs, N=O). ANAL. Calcd for $C_{18}H_{18}N_6O_4S$: C, 52.17%; H, 4.35%; N, 20.29%. Found: C, 52.36%; H, 4.21%; N, 20.42%.

The chemical reaction routes of chromophores a, b, and c are shown in Figure 1.

Synthesis of the polyurethanes

Synthesis of polyurethane Ia

A 50-mL, two-necked, round-bottom flask containing chromophore a (0.20 g, 0.6 mmol) was connected to a reflux condenser and purged with nitrogen for 20 min to remove the atmospheric moisture. To this flask, 5 mL of dry DMF and 1 equiv (0.08 mL, 0.65 mmol) of TDI were added, and the reaction mixture was heated to 110°C and maintained at this temperature for 5 h. The viscous solution was allowed to cool to the ambient temperature, and it was then poured into cold water. The resulting precipitate was filtered and washed several times with water. Subsequently, the precipitate was dissolved in DMF and reprecipitated by the addition of methanol to remove the monomer and low-molecular-weight oligomers. The deep blue compound was filtered and dried in a vacuum desiccator to give polyurethane Ia.

^{1}H-NMR (DMSO-d_6, δ): 2.06–2.16 (m, 3H), 3.91 (br s, 8H), 6.79–7.05 (m, 5H), 7.97 (d, 2H), 8.58 (s, 1H), 8.94 (s, 1H), 9.05 (s, 1H). FTIR (KBr, cm^{-1}): 3388 (br, N—H), 1716 (s, C=O), 1600 (s, N=N), 1516, 1337 (vs, N=O). ANAL. Calcd for $(C_{22}H_{21}N_7O_6S)_n$: C, 51.66%; H, 4.11%; N, 19.18%. Found: C, 51.38%; H, 4.03%; N, 19.07%.

A similar procedure was followed for the syntheses of polyurethanes Ib, Ic, IIa, IIb, and IIc.

Synthesis of polyurethane Ib

^{1}H-NMR (DMSO-d_6, δ): 2.14 (s, 3H), 3.67–4.28 (m, 8H), 6.78–8.23 (m, 10H), 8.45 (s, 1H), 9.04 (s, 1H).
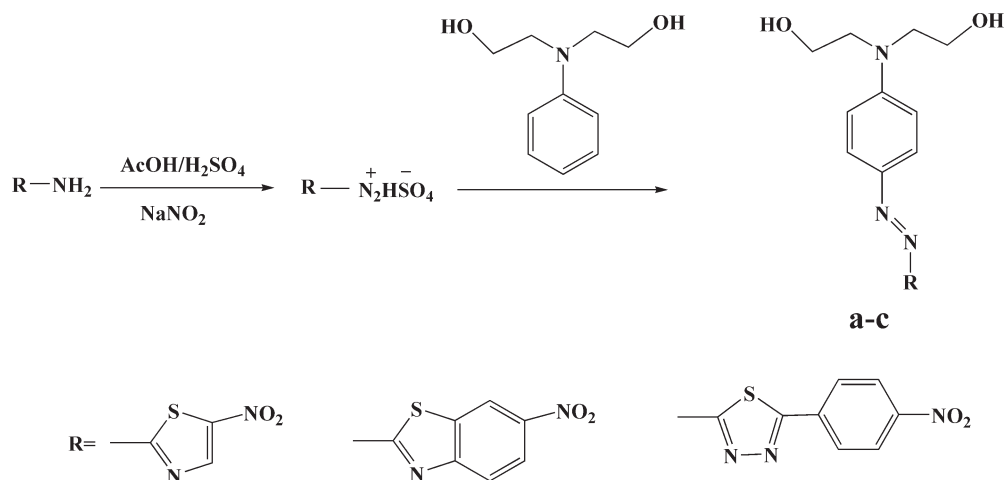
Figure 1 Synthetic routes for the chromophores.

FTIR (KBr, cm^{-1}): 3338 (br, N—H), 1652 (s, C=O), 1600 (s, N=N), 1538, 1332 (vs, N=O). ANAL. Calcd for (C$_{26}$H$_{23}$N$_7$O$_6$S)$_n$: C, 55.61%; H, 4.10%; N, 17.47%. Found: C, 55.78%; H, 3.97%; N, 17.33%.

Synthesis of polyurethane Ic

^{1}H-NMR (DMSO-d_6, δ): 2.08 (s, 3H), 3.34 (br s, 4H), 3.66 (s, 4H), 7.02–8.18 (m, 7H), 8.36 (m, 4H), 8.53–9.60 (s, 2H). FTIR (KBr, cm^{-1}): 3379 (br, N—H), 1707 (s, C=O), 1599 (s, N=N), 1523, 1345 (vs, N=O). ANAL. Calcd for (C$_{27}$H$_{24}$N$_8$O$_6$S)$_n$: C, 55.10%; H, 4.08%; N, 19.05%. Found: C, 55.24%; H, 4.25%; N, 19.28%.

Synthesis of polyurethane IIa

^{1}H-NMR (DMSO-d_6, δ): 2.06 (s, 2H), 3.78–4.27 (m, 8H), 7.08–7.82 (m, 12H), 8.50 (s, 1H), 8.82–9.55 (s, 2H). FTIR (KBr, cm^{-1}): 3384 (br, N—H), 1712 (s, C=O), 1599 (s, N=N), 1519, 1344 (vs, N=O). ANAL. Calcd for (C$_{28}$H$_{25}$N$_7$O$_6$S)$_n$: C, 57.24%; H, 4.26%; N, 16.69%. Found: C, 57.05%; H, 4.15%; N, 16.81%.

Synthesis of polyurethane IIb

^{1}H-NMR (DMSO-d_6, δ): 2.08 (s, 2H), 3.79 (br s, 4H), 3.84 (br s, 4H), 7.07–8.11 (m, 15H), 8.67 (s, 1H), 8.96–9.14 (s, 2H). FTIR (KBr, cm^{-1}): 3459 (br, N—H), 1651 (s, C=O), 1598 (s, N=N), 1510, 1329 (vs, N=O). ANAL. Calcd for (C$_{32}$H$_{27}$N$_7$O$_6$S)$_n$: C, 60.28%; H, 4.24%; N, 15.38%. Found: C, 60.08%; H, 4.10%; N, 15.16%.

Synthesis of polyurethane IIc

^{1}H-NMR (DMSO-d_6, δ): 2.08 (s, 2H), 3.66–4.31 (m, 8H), 3.84 (br s, 4H), 7.07–7.82 (m, 12H), 8.22–8.35 (m,

4H), 8.51–9.57 (s, 2H). FTIR (KBr, cm^{-1}): 3395 (br, N—H), 1681 (s, C=O), 1598 (s, N=N), 1520, 1339 (vs, N=O). ANAL. Calcd for (C$_{33}$H$_{28}$N$_8$O$_6$S)$_n$: C, 59.64%; H, 4.21%; N, 16.87%. Found: C, 59.76%; H, 4.13%; N, 16.76%.

The chemical reaction routes for all the polyurethanes are presented in Figure 2.

RESULTS AND DISCUSSION

Synthesis and characterization of the chromophores

The new NLO chromophores containing thiazole, benzothiazole, and thiadiazole were synthesized via an azo-coupling reaction of 2-amino-5-nitrothiazole, 2-amino-6-nitrobenzothiazole, or 2-amino-5-(4-nitrophenyl)-1,3,4-thiadiazole, respectively, with *N*-phenyldiethanolamine. The resulting chromophores were purified with column chromatography. The reaction pathway for the synthesis of the chromophores is illustrated in Figure 1. The chemical structure of the chromophores was confirmed with FTIR, ^{1}H-NMR, UV–vis, and elemental analyses. FTIR spectra, illustrated in Figure 3, clearly show the characteristic hydroxyl group stretching around 3400 cm^{-1} and the azo-group stretching around 1596 cm^{-1}. The strong bands around 1509 and 1323 cm^{-1} were assigned to asymmetric and symmetric stretching of a nitro group, respectively, signifying the presence of an azo-group in the structure. The assigned peaks are consistent with the proposed structures. The DMF solutions of chromophores **a**, **b**, and **c** showed strong UV absorption maxima around 583, 541, and 544 nm, respectively. The analytical data also confirmed the expected chemical structures. These chromophores were soluble in many organic solvents such as acetone, THF, cyclohexanone, DMF, *N,N*-dimethylacetamide (DMAc), dimethyl
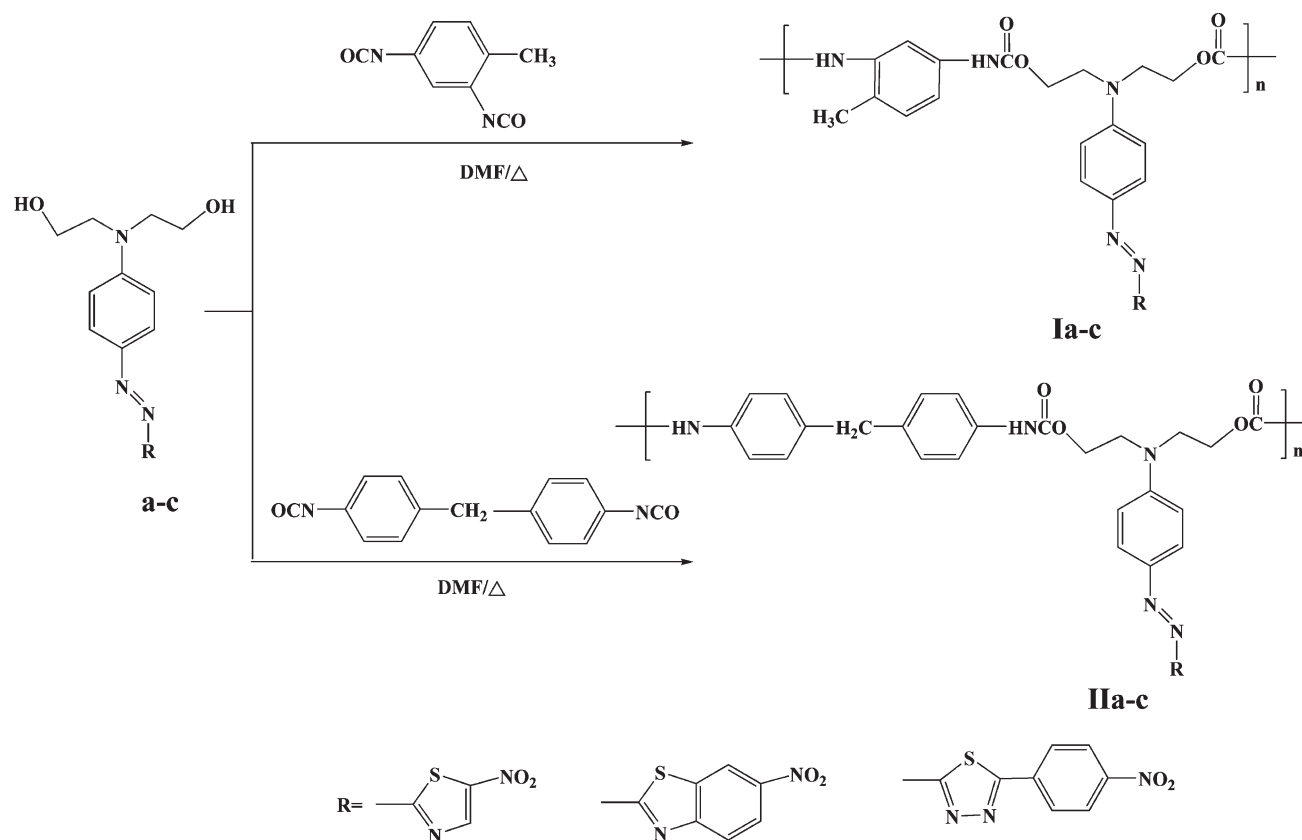
Figure 2 Synthetic routes for the polyurethanes.

sulfoxide (DMSO), and N-methyl-2-pyrrolidinone (NMP).

These NLO chromophores were push–pull-type compounds (see Fig. 1) with the hydroxyl group as the electron donor and the nitro group as the electron acceptor linked through an azo-conjugated bridge.

Synthesis and characterization of the polyurethanes

Chromophores **a**, **b**, and **c** were condensed with TDI (**I**) and MDI (**II**) in a dry DMF solvent to yield polyurethanes (see Fig. 2). The structures of the obtained polyurethanes were confirmed with FTIR, ^{1}H-NMR, GPC, and elemental analyses. In FTIR spectra of the polyurethanes (Fig. 3), a characteristic band near 1700 cm^{-1} was attributed to C=O stretching and indicated the presence of a urethane bond. The strong band around 3380 cm^{-1} was attributed to the N—H stretching. The N—H stretching was broad, and this suggested that the urethane linkages underwent hydrogen bonding. The characteristic bands of symmetrical and asymmetrical stretching vibrations of the nitro groups were also evident at approximately 1520 and 1340 cm^{-1}, respectively, indicating clearly the presence of the NLO chromophore in the polyurethanes.

The chemical shifts of all the polyurethanes were consistent with the proposed structures. The polyurethanes showed signal broadening due to
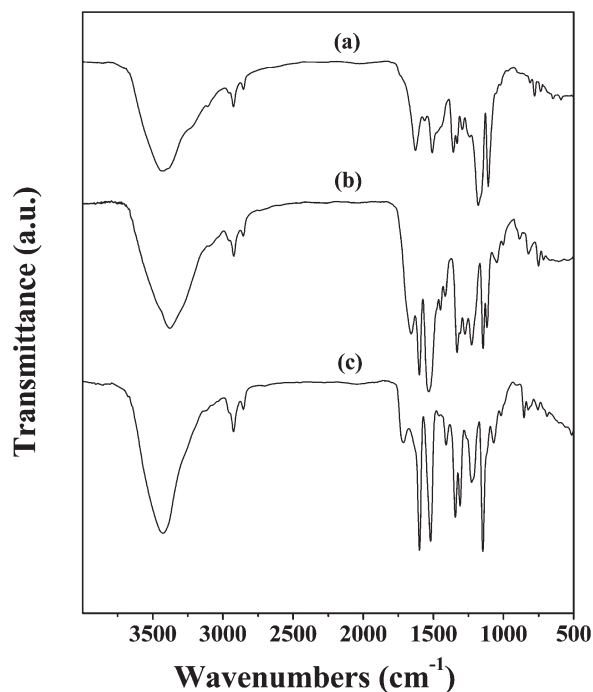

Figure 3 FTIR spectra of (a) chromophore **a**, (b) polyurethane **Ib**, and (c) polyurethane **IIc**.

TABLE I
Physical and NLO Properties of Polyurethanes

Polyurethane	M_n[a]	M_w[a]	λ_{max} (nm)[b]	T_g (°C)	T_d (°C)[c]	T_{opt} (°C)[d]	Φ[e]	Film thickness (μm)	d_{33} (pm/V)
Ia	12,200	25,400	482	169	211	165	0.51	0.09	67.29
IIa	11,100	21,000	362	166	200	160	0.12	0.08	80.80
Ib	11,600	23,200	538	200	259	195	0.21	0.08	84.02
IIb	11,400	19,500	347	188	245	185	0.34	0.07	101.83
Ic	13,000	28,000	506	204	246	200	0.17	0.08	96.67
IIc	10,700	22,500	538	195	243	190	0.21	0.07	105.45

[a] Measured by GPC in THF with a PS standard.
[b] Polymer film after corona poling.
[c] Decomposition temperature measured with TGA at 10 wt % under the protection of N_2 at a scan rate of 10°C/min.
[d] Maximum SHG value measured with *in situ* poling as a function of temperature.
[e] Order parameter.

polymerization. The resonances in the range of 8.50–9.60 ppm were assigned to the amine protons, indicating the formation of a urethane linkage. The molecular weights of the polyurethanes were determined by GPC with PS as the standard and THF as the eluent, and the data are presented in Table I. The polydispersities were in the range of 1.71–2.15. The elemental analysis data fit the polyurethane structures. The analytical and spectral data were consistent with the proposed polyurethane structures. The polyurethanes were soluble in many common organic solvents such as acetone, THF, cyclohexanone, DMF, DMAc, DMSO, and NMP. These polyurethanes offered good processability; hence optical-quality thin films could be easily prepared from their solutions.

Thermal properties of the polyurethanes

The thermal behavior of the polyurethanes was investigated to determine T_g and the thermal degradation pattern with DSC and TGA. The results are summarized in Table I. From the DSC traces (Fig. 4), it was observed that the T_g values of the polyurethanes were in the range of 166–204°C, depending on the structures of the NLO chromophores attached to the polyurethane backbone. Among the polyurethanes, chromophores containing the thiazole moiety (**Ia** and **IIa**) exhibited lower T_g values in comparison with those of the chromophores containing benzothiazole and thiadiazole moieties (**Ib**, **IIb**, **Ic**, and **IIc**). This may be due to the small size of the thiazole moiety in the polyurethane matrix. On the other hand, polyurethanes containing TDI backbones exhibited higher T_g values than the polyurethanes containing MDI backbones. This could be attributed to the enhanced chain rigidity caused by the incorporation of the toluene ring. Among the polyur-

ethanes, **Ic** exhibited a very high T_g (~204°C), which reflected the stable NLO azo-thiadiazole structure.

A differential branching structure analysis (TGA) of the obtained polyurethanes was carried out, and the resulting thermograms are presented in Figure 5. From the TGA traces, it was observed that polyurethanes containing benzothiazole and thiadiazole chromophores exhibited better thermal stability than polyurethanes containing the thiazole chromophore. At higher temperatures, **Ic** exhibited a higher value, which reflected the increased thermal stability among the polyurethanes. Thermal decomposition temperatures were calculated at the 10 wt % loss, and the values so obtained are included in Table I.
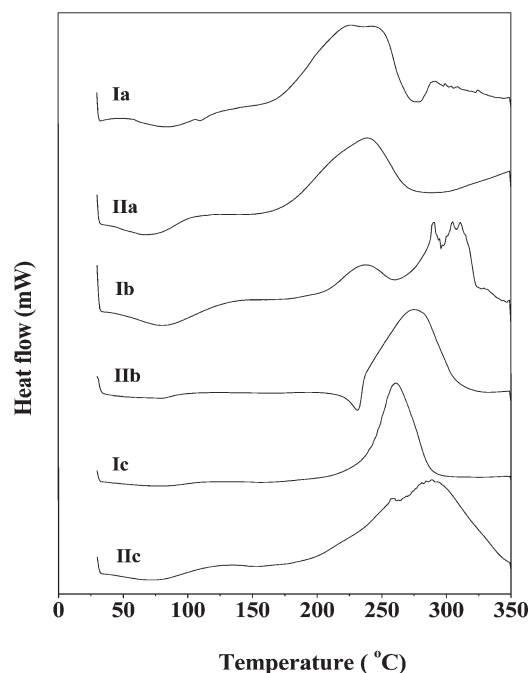

Figure 4 DSC thermograms of the polyurethanes at a heating rate of 10°C/min under a nitrogen atmosphere.
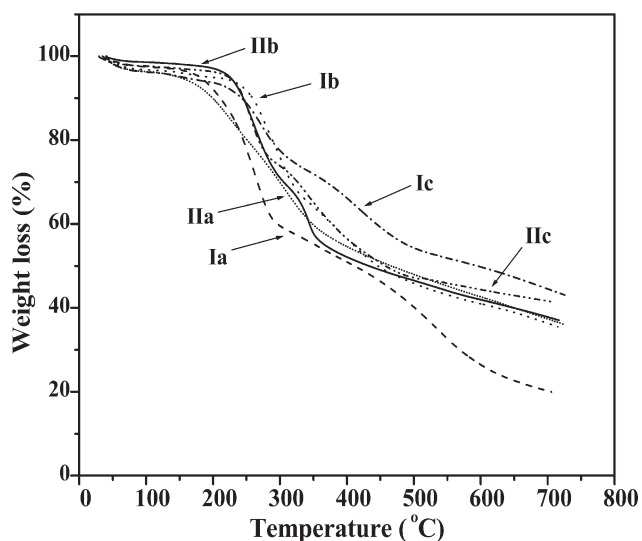
Figure 5 TGA thermograms of the polyurethanes at a heating rate of 10°C/min under a nitrogen atmosphere.

Figure 6 SHG signals of polyurethane **IIc** (used to determine T_{opt}) as a function of temperature.

From both TGA and DSC patterns, it was observed that all the polyurethanes underwent decomposition above 200°C, which was far from their corresponding T_g values. This is the reason that the poling carried out near the T_g values (± 10°C) was more appropriate and did not damage the films of the NLO chromophores.

NLO properties of the polyurethanes

The noncentrosymmetric alignment of the NLO chromophores in the polyurethane films could be achieved by corona poling at a temperature close to T_g. To select the suitable temperature to obtain maximum SHG values, the *in situ* poling for all the polyurethanes as a function of temperature was carried out. A typical profile of the *in situ* poling experiments with polyurethane **IIc** is presented in Figure 6. As the voltage was turned on, an SHG signal could be observed, even at room temperature. Upon further heating, the SHG signal increased until it approached the T_g value. The SHG signal was maximum at 190°C and decreased subsequently. Furthermore, the SHG signal was higher during the cooling stage because of a decrease in thermal randomization. The measured maximum SHG temperatures for the remaining polyurethanes are included in Table I. To determine the poling efficiency, we measured the absorption spectra of all the polyurethanes before and after poling. Typical UV–vis absorption spectra of polyurethane **Ib** before and after poling are presented in Figure 7. After the electric poling, the dipole moments of the NLO chromophores were aligned along the direction of the applied electric field, and as a result, the UV–vis spectrum of the
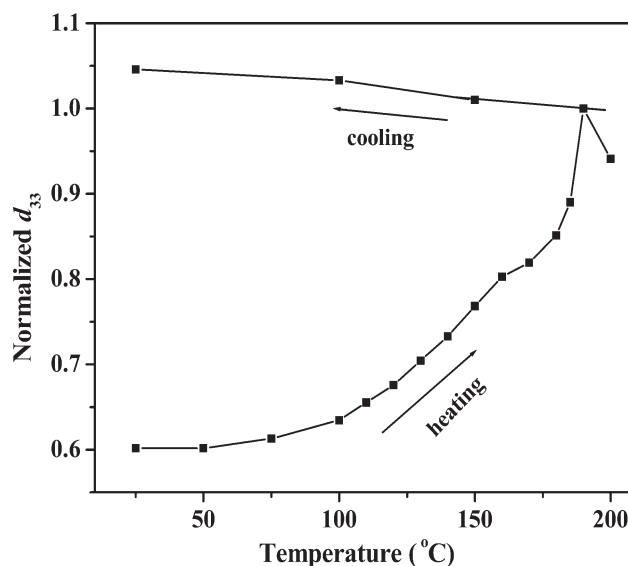
polyurethane exhibited a blueshift and a decrease in absorption due to birefringence. From the change in the absorbance, the order parameter of the poled film, which was related to the poling efficiency, was estimated. The order parameter of poled polyurethane film **Ib** (order parameter $= 1 - A_1/A_0$, where A_0 and A_1 are the absorbances of the polymer film before and after poling, respectively) was found to be 0.21. The estimated order parameters of the remaining polyurethane films are given in Table I. All these data suggest that the polyurethanes were efficiently poled, and as a result, the chromophores were effectively aligned because the order parameter described the chromophore alignment and correlated to the NLO properties of the polyurethanes. The
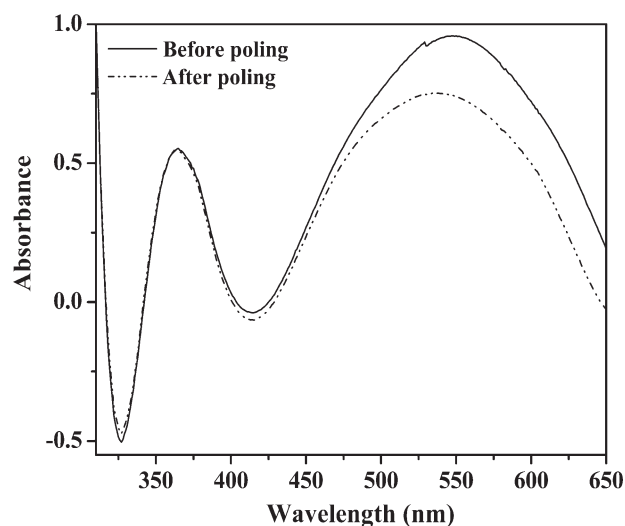

Figure 7 UV–vis absorption spectra of polyurethane **Ib** before and after poling.
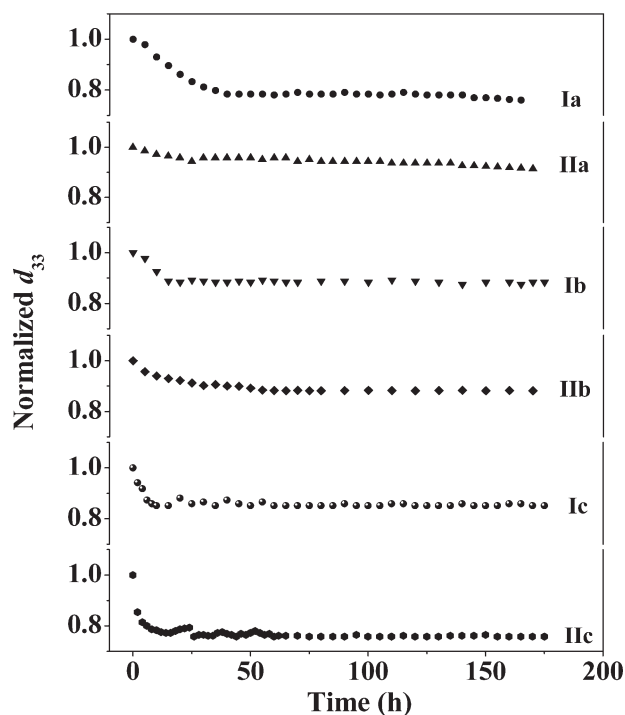
Figure 8 Temporal stability of the SHG signals of the polyurethanes at 125°C in air.

poling was carried out by the application of a voltage of 3 kV through a corona needle for 1 h at 165, 195, 200, 160, 185, and 190°C for polyurethanes **Ia**, **Ib**, **Ic**, **IIa**, **IIb**, and **IIc**, respectively.

The second-order NLO coefficient (d_{33}) for the poled polyurethane was calculated on the basis of the following equation:[42]

$$\frac{d_{33,s}}{d_{36,k}} = \frac{\chi_s^{(2)}}{\chi_k^{(2)}} = \sqrt{\frac{I_s}{I_k}} \frac{l_{c,k}}{l_s} F$$

where $\chi_s^{(2)}$, $\chi_k^{(2)}$ are the second-order susceptibilites of polyurethane sample and KDP crystal, respectively; $d_{33,s}$ and $d_{36,k}$ respectively denote the second-order NLO coefficients of polyurethane sample and KDP crystal; $d_{36,k}$ is the d_{36} value of the KDP crystal (0.40 pm/V); I_s and I_k are the SHG intensities of the polyurethane sample and the KDP crystal, respectively; $l_{c,k}$ is the coherence length of the KDP crystal (11.4 μm); l_s is the thickness of the polyurethane sample; and F is the correction factor, which is equal to approximately 1.2 when $l_{c,k} \gg l_s$. The calculated d_{33} values of these polyurethanes at the wavelength of 1064 nm are included in Table I. All the polyurethanes exhibited d_{33} values in the range of 67.29–105.45 pm/V, and this signified that the polyurethanes showed an enhanced resonance effect due to high absorption at 532 nm with reference to a 1.0-mm-thick KDP crystal. The d_{33} values reported here are far superior to the data reported for dialky-

laminonitrostilbene-substituted NLO polyurethane systems.[31,43]

The relaxation process of dipole orientation is related directly to T_g, and a higher T_g value implies higher orientational stability. To probe this stability, the temporal and thermal stability of the SHG signals for all the polyurethanes was monitored, and the data generated as a function of time are presented in Figure 8. At room temperature, all the polyurethanes were stable, and there was no decay in the intensity of the SHG signal. However, at 125°C in air, after an initial decay to approximately 88% of the original signal, more than 85% of the SHG signal remained stable after 170 h for polyurethane **IIb**, as can be seen in Figure 8.

To determine the high-temperature stability of the polyurethanes, the temporal stability of the SHG signal for all the polyurethanes was studied. Figure 9 displays the thermal endurance of the nonlinear activity of poled polyurethane **Ib**. To investigate the real time of NLO decay, the SHG signal was monitored with a stepwise rise in the temperature from the ambient temperature to 220°C. At a temperature near 160°C, the SHG signal started to decrease rapidly. High thermal stability was observed up to approximately 160°C. This improved stability of the induced dipole alignment could be attributed to the hydrogen bonding. The hydrogen bonds in polyurethanes, polyamides, polypeptides, and so forth are well known and have been studied extensively,[44–46] and they are known to increase the rigidity of the polymer system while suppressing the relaxation of aligned dipoles. Because our polyurethane systems were completely amorphous, the high entropy conformation of the backbone chain allowed the
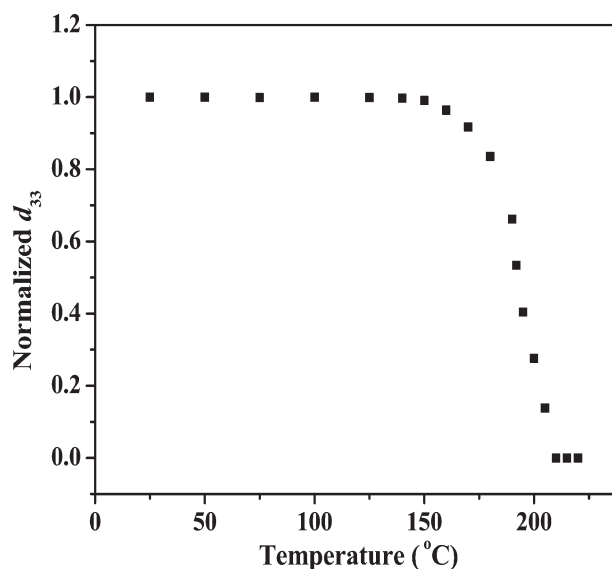

Figure 9 SHG signals of polyurethane **Ib** as a function of temperature.

hydrogen bonding to take place more freely. Thus, when our systems were compared with other systems with similar structures and T_g values, such as poly(methyl methacrylate) (PMMA)- or PS-based NLO polymers, in which hydrogen bonding does not occur, better stability was observed. A discussion of the stability of PMMA- and PS-based NLO polymers can be found in the literature.[47–49] Figure 9 further shows that the signal disappeared completely as the temperature rose above T_g. However, the same magnitude of the SHG signal was recovered from this sample after it was repoled by corona discharging, and this indicated that the NLO chromophore was not damaged after experiencing a high temperature. Similar results were observed in the remaining polyurethanes (**Ia**, **Ic**, **IIa**, **IIb**, and **IIc**). The thermal characteristics and optical nonlinearities of these polyurethanes clearly indicated that these could be useful in device applications.

CONCLUSIONS

NLO active polyurethanes with azo-chromophores containing nitrothiazole, nitrobenzothiazole, and nitrothiadiazole moieties in the side chain were synthesized and characterized. The analytical and spectral data were consistent with the proposed structures of the chromophores and polyurethanes. The polyurethanes displayed very good solubility in many common organic solvents and exhibited good thermal stability, which was confirmed by TGA. Among the polyurethanes, chromophores containing a nitrothiazole moiety exhibited lower T_g values in comparison with chromophores containing nitrobenzothiazole and nitrothiadiazole moieties. This was attributed to the small size of the nitrothiazole moiety in the polyurethane matrix. The polyurethanes having TDI backbones demonstrated relatively high T_g values in comparison with those polyurethanes having MDI backbones. This was due to the enhancement of the rigidity caused by the incorporation of the toluene ring. Because of the high solubility of the polyurethanes, these could be easily processed into high-optical-quality thin films for device applications. After orientation of the dipoles, the second-order optical nonlinearity and thermal stability were enhanced significantly, and large d_{33} values ranging from 67.29 to 105.45 pm/ V were exhibited because of the high absorption at 532 nm. High thermal endurance of the poled dipoles was observed for all the polyurethanes. This was explained by the formation of extensive hydrogen bonds between urethane linkages, which are known to increase the rigidity of the polymer matrix, thus preventing the relaxation of induced dipoles.

References

1. Casalboni, M.; Caruso, U.; De Maria, A.; Fusco, M.; Panunzi, B.; Quatela, A.; Roviello, A.; Sarcinelli, F.; Sirigu, A. J Polym Sci Part A: Polym Chem 2004, 42, 3013.
2. Hua, J. L.; Li, Z.; Long, K.; Qin, J. G.; Li, S. J.; Ye, C.; Lu, Z. H. J Polym Sci Part A: Polym Chem 2005, 43, 1317.
3. Briers, D.; Koeckelberghs, G.; Picard, I.; Verbiest, T.; Persoons, A.; Samyn, C. Macromol Rapid Commun 2003, 24, 841.
4. Balakrishnan, M.; Faccini, M.; Diemeer, M. B. J.; Verboom, W.; Driessen, A.; Reinhoudt, D. N.; Leinse, A. Electron Lett 2006, 42, 51.
5. Kim, S. K.; Hung, Y. C.; Seo, B. J.; Geary, K.; Yuan, W.; Bortnik, B.; Fetterman, H. R.; Wang, C.; Steier, W. H.; Zhang, C. Appl Phys Lett 2005, 87, 061112-1-2.
6. Park, S.; Ju, J. J.; Park, S. K.; Lee, M. H.; Do, J. Y. Appl Phys Lett 2005, 86, 071102-1-3.
7. Sakai, W.; Chiga, K.; Tsutsumi, N. J Polym Sci Part B: Polym Phys 2001, 39, 247.
8. Katti, K. V.; Raghuraman, K.; Pillarsetty, N.; Karra, S. R.; Gulotty, R. J.; Chartier, M. A.; Langhoff, C. A. Chem Mater 2002, 14, 2436.
9. Hao, J.; Han, M. J.; Guo, K.; Zhao, Y.; Qiu, L.; Shen, Y.; Meng, X. Mater Lett 2008, 62, 973.
10. Carella, A.; Castaldo, A.; Centore, R.; Fort, A.; Sirigu, A. J Chem Soc Perkin Trans 2002, 2, 1791.
11. Batista, R. M. F.; Costa, S. P. G.; Belsley, M.; Raposo, M. M. Tetrahedron 2007, 63, 9842.
12. Rao, V. P.; Jen, A. K. Y.; Wong, K. Y.; Drost, K. J. Tetrahedron Lett 1993, 11, 34.
13. Abbotto, A.; Bradamante, S.; Facchetti, A.; Pagani, G. A. J Org Chem 1997, 17, 5755.
14. Yuquan, S.; Yuxia, Z.; Zao, L.; Jianghong, W. Q.; Ling, L.; Shixiong, Z.; Jianfeng, Z.; Jiayun, J. J Chem Soc Perkin Trans 1999, 1, 3691.
15. Dirk, C. W.; Katz, H. E.; Schilling, M. L.; King, L. A. Chem Mater 1990, 2, 700.
16. Leng, W. N.; Zhou, Y. M.; Xu, Q. H.; Liu, J. Z. J Polym 2001, 42, 9253.
17. Centore, R.; Tuzi, A.; Panunzi, B. Kristallogr Z 1997, 212, 890.
18. Ambrosanio, P.; Centore, R.; Concilio, S.; Panunzi, B.; Sirigu, A.; Tirelli, N. J Polym 1999, 40, 4923.
19. Lee, J. Y.; Bang, H. B.; Park, E. J.; Rhee, B. K.; Lee, S. M.; Lee, J. H. J Polym Sci Part A: Polym Chem 2004, 42, 3189.
20. Zhu, P.; Van der Boom, M. E.; Kang, H.; Evmenenko, G.; Dutta, P.; Marks, T. J. Chem Mater 2002, 14, 982.
21. Li, Z.; Hua, J.; Li, Q.; Huang, C.; Qin, A.; Ye, C.; Qin, J. Polymer 2005, 46, 11940.
22. Dudkina, M.; Aseev, V.; Temkovtsev, A.; Tenhu, H. J Polym Sci Part B: Polym Phys 2005, 43, 398.
23. Qin, A.; Yang, Z.; Bai, F.; Ye, C. J Polym Sci Part A: Polym Chem 2003, 41, 2846.
24. Lu, J.; Yin, J. J Polym Sci Part A: Polym Chem 2003, 41, 303.
25. Reddy, S. D.; Shu, C. F.; Wu, F. I. J Polym Sci Part A: Polym Chem 2002, 40, 262.
26. Hsiao, S. H.; Chem, Y. J. Eur Polym J 2002, 38, 815.
27. Xu, J.; He, C.; Chung, T. S. J Polym Sci Part A: Polym Chem 2001, 39, 2998.
28. Saadeh, H.; Wang, L.; Yu, L. Macromolecules 2000, 33, 1570.
29. Sakai, Y.; Ueda, M.; Fukuda, T.; Matsuda, H. J Polym Sci Part A: Polym Chem 1999, 37, 1321.
30. Ballet, W.; Verbiest, T.; Beylen, M. V.; Persoons, A.; Samyn, C. Eur Polym J 2001, 37, 2419.

31. Lee, J. Y.; Bang, H. B.; Park, E. J.; Baek, C. S.; Rhee, B. K.; Lee, S. M. Synth Met 2004, 144, 159.

32. Caruso, U.; Casalboni, M.; Fort, A.; Fusco, M.; Panunzi, B.; Quatela, A.; Roviello, A.; Sarcinelli, F. Opt Mater 2005, 27, 1800.

33. Lee, J. Y.; Bang, H. B.; Baek, C. S. Synth Met 2005, 148, 161.

34. Lee, J. Y.; Lee, W. J.; Park, E. J.; Bang, H. B.; Rhee, B. K.; Jung, C.; Lee, S. M.; Lee, J. H. Bull Korean Chem Soc 2003, 24, 1727.

35. Woo, H. Y.; Lee, K. S.; Shim, H. K. Polym J 2000, 32, 8.

36. Lee, J. Y.; Park, E. J.; Lee, H.; Rhee, B. K. J Polym Sci Part A: Polym Chem 2002, 40, 1742.

37. Lee, J. Y.; Park, E. J.; Lee, H.; Rhee, B. K. Polym Bull 2002, 48, 233.

38. Park, C. K.; Zieba, C. F.; Zhao, C. F.; Swedek, B.; Wijekoon, W. M. K. P.; Prasad, P. N. Macromolecules 1995, 28, 3713.

39. Tsutsumi, N.; Yoshizaki, S.; Sakai, W.; Kiyotsukuri, T. Macromolecules 1995, 28, 6437.

40. Tambe, S. M.; Kittur, A. A.; Inamdar, S. R.; Mitchell, G. R.; Kariduraganavar, M. Y. Opt Mater, 2009, 31, 817.

41. Foroumadi, A.; Daneshtalab, M.; Shafiee, A. Arzneim-Forsch 1999, 49, 1035.

42. Dalton, L. R.; Xu, C.; Harper, A. W.; Ghosn, R.; Wu, B.; Liang, Z.; Montgomery, R.; Jen, A. K. Y. Nonlinear Opt 1995, 10, 383.

43. Woo, H. Y.; Shim, H. K.; Lee, K. S. Macromol Chem Phys 1998, 199, 1427.

44. Bonart, R. J Macromol Sci Phys 1968, 2, 115.

45. Seymour, R. B. Polymer Chemistry, 2nd ed.; Marcel Dekker: New York, 1998; p 175.

46. Lin, S. B.; Kwang, K. S.; Tsay, S. Y.; Cooper, S. L. Colloid Polym Sci 1995, 263, 128.

47. Ye, C.; Marks, T. J.; Yang, J.; Wong, G. K. Macromolecules 1987, 20, 2322.

48. Robello, D. R.; Dao, P. T.; Schildkraut, J. S.; Scozzafava, M.; Urankar, E. J.; Willand, C. S. Chem Mater 1995, 7, 284.

49. Joglekar, B.; Shibata, K.; Muramatsu, H.; Matsui, M.; Hirota, K.; Hosoda, M.; Tai, K. Polym J 1997, 29, 184.